International Journal of Occupational Safety and Ergonomics

ISSN: (Print) (Online) Journal homepage: https://www.tandfonline.com/loi/tose20

Development of an algorithm for effective design of respirator half-masks and encapsulated particle filters

Serhii Cheberyachko, Yurii Cheberyachko, Mykola Naumov & Oleg Deryugin

To cite this article: Serhii Cheberyachko, Yurii Cheberyachko, Mykola Naumov & Oleg Deryugin (2021): Development of an algorithm for effective design of respirator half-masks and encapsulated particle filters, International Journal of Occupational Safety and Ergonomics, DOI: 10.1080/10803548.2020.1869429

To link to this article: https://doi.org/10.1080/10803548.2020.1869429

Published online: 25 Feb 2021.

International Journal of Occupational Safety and Ergonomics (JOSE), 2021
https://doi.org/10.1080/10803548.2020.1869429

Development of an algorithm for effective design of respirator half-masks and encapsulated particle filters

Serhii Cheberyachko *, Yurii Cheberyachko, Mykola Naumov and Oleg Deryugin

Dnipro University of Technology, Ukraine

Objective. Social and economic situations in the modern world require new approaches to the development of respiratory protective equipment. This study aimed to improve the three-dimensional modeling process for respirator half-masks and encapsulated particle filters. *Methods.* Basic provisions of the theory of non-stationary filtration and hydroaerodynamics, the Nelder–Mead method and the linear interpolation equation were used. *Results.* The peculiarity of the algorithm is the adjustment stage of the design process aimed at checking efficiency of the half-mask. The surface of the half-mask was constructed according to the coordinates of a three-dimensional model of a worker's head. *Conclusion.* For the first time, the regularities of an algorithm for designing the half-mask surface of dust respirators were defined based on the data for three-dimensional coordinates of key points of anthropometric parameters of workers' faces. The pressure difference on the encapsulated particle filters of dust respirators is determined by the particle filter's resistance coefficient and air flow through them, and the diameter ratio of their outlets and inlets. The developed algorithm provides product verification at the design stage using criteria evaluating parameters of a polygonal model of the head, preliminary calculation of the protection factor and checking the tightness of the prototype.

Keywords: algorithm; model; half-mask; dust respirator; obturator; coefficient of insulation

1. Introduction

One of the significant harmful production factors is dust in the air of the working area. To solve the problem of creating safe working conditions, it is necessary to develop energy-saving and resource-saving technologies that will ensure the localization of dust emissions in the places of their formation, cleaning dusty air using built-in devices and those attached to the working tools, and further dust collection in air treatment facilities. Unfortunately, the use of such measures in some cases is not possible, and in some cases requires significant financial costs to introduce new safe dust collection technology. Therefore, respiratory protective devices – dust respirators – remain the main type of protection for workers performing production functions in the relevant working conditions. However, they may have certain disadvantages that lead to a deterioration in the degree of protection of workers [1]; in particular, the low duration of protective action in conditions of heavy physical labor and, as a consequence, high initial breathing resistance [2]. This is due to the design of the encapsulated particle filter of the dust respirator, which has a small outlet and a flat rear wall to which the corrugated particle filter is adjacent. In dusty conditions, this design leads to a rapid increase in the pressure drop due to the uneven air load over the particle filter area. So, a portion of the air that passes through the particle filter in front of the outlet of the encapsulated particle filter freely enters the space under the mask, and the other portion of the air permeates between the rear wall of the box and the particle filter corrugations, i.e., to get to the outlet it needs to overcome the additional resistance of the particle filter corrugations that are adjacent to the rear wall, which leads to a reduction in the protective action of the dust respirator. On the other hand, the protective properties of dust respirators depend on a reliable fit to a worker's face behind the obturation line. Most experts tend to think that the main reason for the low insulating properties of half-masks of dust respirators is the diversity of anthropometric characteristics of the worker's face. Most often, gaps are formed in the area of the nose bridge of a worker's face [3]. Thus, checks of protective properties of dust respirator half-masks demonstrated the worst results during conversations and head tilts, and change of facial expressions of a worker when performing his professional functions [4]. Therefore, the question of developing an algorithm for designing the dust respirator half-mask is an urgent task today.

The algorithm for manufacturing dust respirator half-masks is a complex process consisting of the development of design documentation, technical specifications, draft and technical design, and working documentation [5]. The implementation of these steps requires a significant amount of time and appropriate professional training. The modern

*Corresponding author. Email: Laboursafoffice@ukr.net

development of the industry constantly demands reduction of this process without loss of quality of the final product. Different approaches are proposed for this purpose, particularly computer-aided design (CAD) systems. However, the process of designing dust respirators is insufficiently formalized and in most cases is based on heuristic methods mainly supported by the designer's erudition and intuition [5–7]. This contributes to the occurrence of errors and loss of time to correct them. Experts consider that the greatest problem is the lack of systematized data taking into account the influence of a technological process on the general quantitative or qualitative regularities of the phenomena taking place in protective devices [8]. It is believed that the development of their appearance takes the most time in the design of half-masks of dust respirators [9]. At the same time, the key objective is to ensure fit of the half-masks to as many workers with different anthropometric characteristics of faces as possible. It is also important to take into account the influence of the working conditions, physical load and psychological effect of respirators, which can decrease the effectiveness of the respiratory protective devices. There is a significant number of publications where the effect of any factor on the quality of a dust respirator is studied in detail [10–15]. For example, a database of anthropometric parameters was created, according to which corresponding tables were made [10,11], the influence of a dust respirator on the physiological state of workers was studied [12], the change of protective efficiency depending on operating conditions was estimated [13,14], etc. This makes it possible to form the structure of dust respirators from different blocks, but the need for experimental verification of prototypes and their improvement arises, which takes a lot of time [15].

The performed studies have shown that in heavy-duty conditions, with high air humidity (>80%) and dust concentration ($\geq$50 mg/m^3), the respiratory protective equipment (RPE) is characterized by frequent replacement of particle filters three or four times per shift because of a rapid increase in respiratory resistance due to the effect of dust 'cementation' following its reaction with exhaled moisture [16,17]. This situation was caused by the design of the dust respirator encapsulated particle filter, which has a small outlet and a flat rear wall to which the corrugated particle filter is adjacent, which in dust conditions leads to a rapid increase in the pressure drop through the unevenness of the air load over the particle filter area [12]. In addition, dust respirators are characterized by a low protection factor because of the suction of unfiltered air in areas where the half-mask fits to a worker's face, which is caused by the uneven distribution of clamping forces along the half-mask obturation line because of the two-point headband fixation on the exhalation valve clip [18,19]. Based on the performed analysis it is possible to define the purpose of scientific research, which is to carry out theoretical research and justify a design algorithm for the structure of a dust respirator half-mask and encapsulated particle filter.

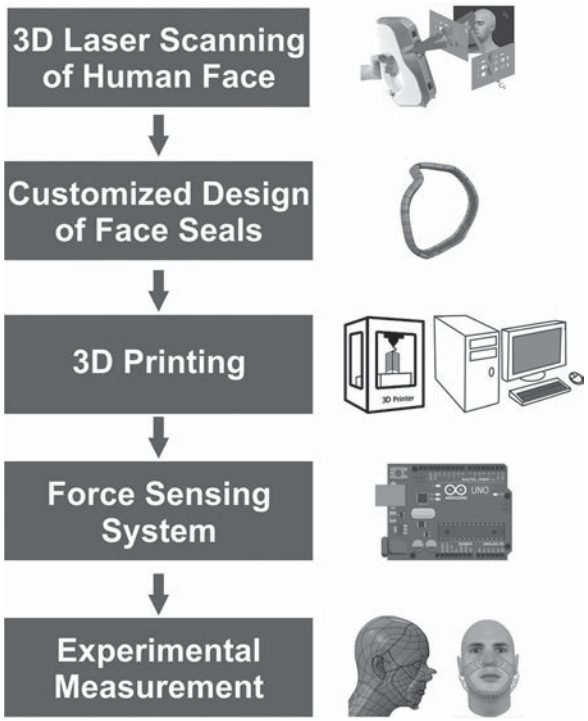

Figure 1. Dust respirator half-mask design and manufacturing algorithm [15]. Note: 3D, three-dimensional.

2. Materials and methods

The generally accepted algorithm for designing and manufacturing half-masks of dust respirators consists of several stages (Figure 1):

- study of anthropometric characteristics of employees' faces by three-dimensional (3D) scanning;
- construction of digital models of heads of workers of several standard sizes;
- development of a 3D surface of a mask/half-mask by means of non-uniform rational basis spline (NURBS) surfaces;
- laboratory verification of compliance of the designed mask/half-mask with the set efficiency criteria;
- selection of the appropriate package of filter materials in accordance with the operating conditions;
- production of experimental samples for laboratory verification of compliance with the requirements of the standards.

To determine the anthropometric dimensions of faces that are peculiar to the workers of a certain region, one may use the parameters provided by Standard No. ISO/TS 16976-2:2015. In the work [20] provided similar studies for the construction of masks or half-masks for personal respiratory protection (Figure 2). Table 1 presents the abbreviations and descriptions of face dimensions according to Figure 2.

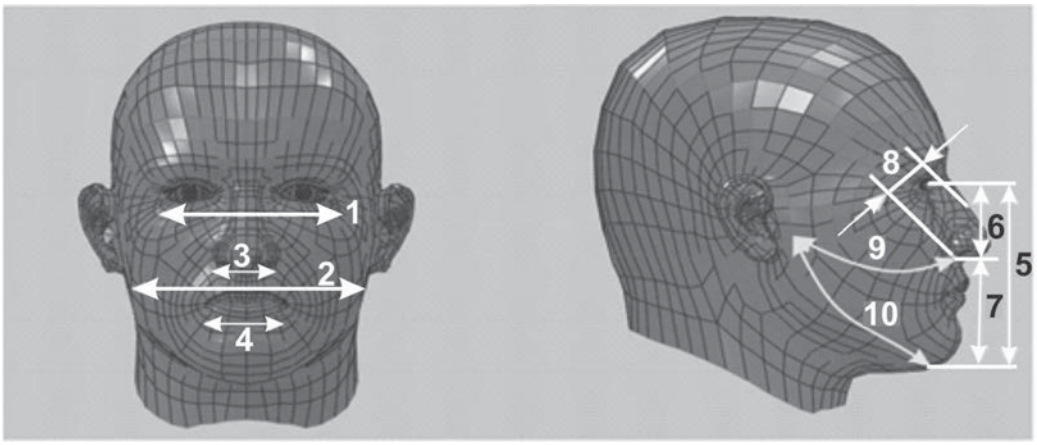

Figure 2. Anthropometric dimensions of a face measured on volunteer workers. Note: See Table 1 for description of dimensions 1–10.

Table 1. Abbreviations and description of face dimensions.

Number*	Abbreviation	Face dimension	Face dimension description
1	GONI	Face width at eye line	The maximum horizontal width of the face between the extreme points of the eye sockets
2	ZYGO	Width of the face at the corners of the lower jaw	The maximum horizontal width of the face between the jaw arches
3	NOSEBRTH	Width of the nose	The distance between the right and left points of the nose wings
4	LIPLGTHH	Length of the lips	The distance between the right and left points behind the corners of the mouth
5	MENSELL	Length of the face	The distance between the lower point of the chin and the upper point of the nose bridge
6	NOSEPRH	Length of the nose	The distance between the lower point of the nose and the upper point of the nose bridge
7	MSNL	Lower part of the face	The distance between the lower point of the chin and the lower point of the nose
8	NOSP	Projection of the nose	The distance from the base of the nose to the chin
9	TRNA	Width of a cheek	The distance from the lower edge of the ear to the wing of the nose
10	TRMA	Width of the cheekbone	The distance from the lower edge of the ear to the chin

*Number corresponds to the dimension in Figure 2.

According to the face parameters, the digital polygonal model of the head was constructed, which allows changing its texture based on defined anthropometric dimensions of a worker's face. To obtain this, the vertices of the applied polygonal grid were linked to the key anthropometric points on the scanned images of the workers' faces, based on which the contours of the obturator were later determined.

To do this, on the scanned images of workers' faces, using the developed software environment and the matrix function of 3D reconstruction, the coordinates of anthropometric points were determined as follows:

$$\begin{pmatrix} x \\ y \\ z \end{pmatrix} = \text{reconstruct}\,(u, v, i, k, P_c, P_p), \qquad (1)$$

where u, v = coordinates of the points determined by the algorithms of analysis of the digital image of a worker's face and the identification of the backlight pattern, which

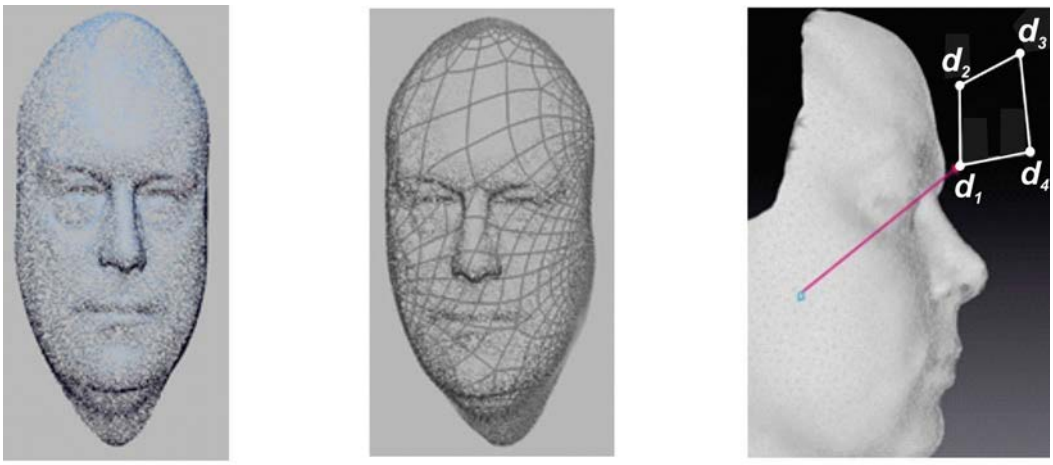

Figure 3. Stages of transformation of the scanned image of a worker's head: from the point cloud (a) with applied splines (b) to a digital view with mark-up and coordinates (c). d_1, d_2, d_3, d_4 = coordinates of a point.

are determined by an array of colored pixels, and allow you to get a set of $\{\mu_k = < (u_k/v_k), i_k >\}$ identified template points; i = index of the template straight line; k = adjustment factor between the data matrices of the scanned images of the workers' faces; P_c, P_p = projection matrices of the filtering camera and projector, determined in the calibration process.

Further, based on the multistage evaluation of the proportions of a worker's head represented by a cloud of points (Figure 3a), using a weighted Gaussian radial function and local fitting taking into account the topological structure, we constructed a digital image. In such a way, the first stage was specified by coordinates $d = (d_1, d_2, \ldots, d_n)$, representing a set of vectors $d_i = (d_1^i, d_2^i, \ldots, d_n^i)$, whose elements are the vertex indices of the polygonal model. The vector defines a broken line that describes one characteristic feature of a worker's face, the contour of the nose, lips or face in general. The dimensions of the lines are set using anthropometric points defined on the worker's face. The lines form a parabolic spline continuously defining the shape of the face (Figure 3b). Each spline is evenly split by additional points to form an equal number of sections on all horizontal lines. The additional points are joined together to form a grid of quadrilaterals (Figure 3c). When fitting the mark-up to anthropometric points, we use three types of transformations: identical, offset relative to established points and links relative to already placed points.

For the 'precise' stages of fitting individual parts of the face, we used the Nelder–Mead method. This approach allows one to work with a wide class of strain models and make edits at any stage in cases of incorrect data entry, with heavily contaminated images and other defects (Figure 4).

The difference between this approach and the known ones is the absence of an intermediate model, which is adjusted to the anthropometric points on the scanned image of the worker's face. In this case, first there is a rough fit using an interactive algorithm, and then the precise one using splines.

The solution to the problem of converting a digital image of a worker's face given in a 3D coordinate system into new parameters of an individual half-mask of a dust respirator can be represented as a transformation:

$$F_0 = \prod (F_n), \tag{2}$$

where F_0 = shape of a worker's face having certain initial values of coordinates *x, y, z* for points 1, 2, 3, ... , n that determine its parameters in a 3D coordinate system; Π = operator of the transformation of key anthropometric points on the worker's face to the geometric parameters of the dust respirator; F_n = shape of the half-mask of a dust respirator, which is determined by a change in the initial values of the coordinates *x, y, z*.

The process of constructing a half-mask of a dust respirator was set by a sequential multilevel transformation of the form and parameters of the digital image of the worker's face, which was separated into several levels with the corresponding split of the design process function into separate subfunctions. To solve this problem, we used the classical method of linear interpolation – construction of a corresponding polynomial, which is set using the Newton form. This approach is based on the Weierstrass theorem, which states that any continuous function on an interval can be uniformly approximated with arbitrary precision by a polynomial. To obtain the equations of the spline surface of the dust respirator half-mask, the function $f(x,y)$ was found, where the grid points given in the table $\{x_i, y_i, i = \overline{1,N}\}$ obtained from the polygonal model of the worker's

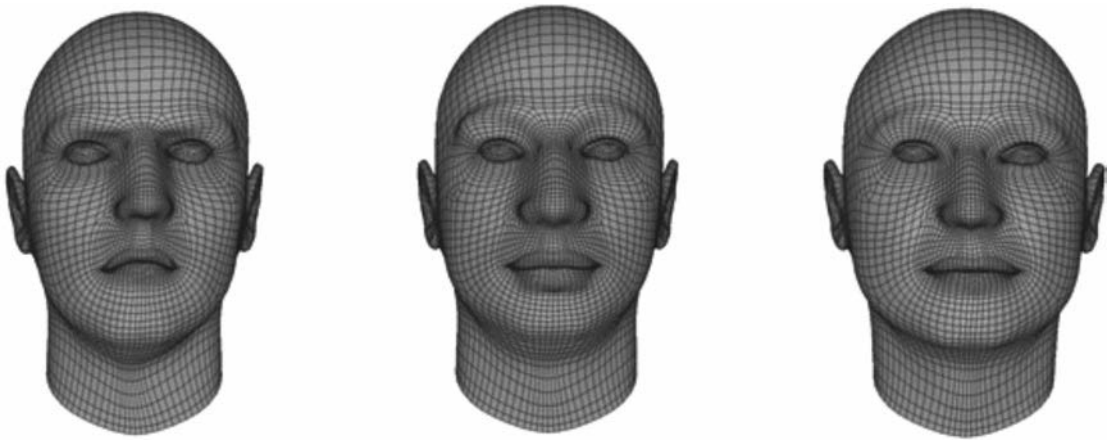

Figure 4. Digital models of a worker's head with different anthropometric parameters.

face are known. After appropriate transformations, the surface of the dust respirator half-mask was described using the following function:

$$\phi(x,y) = \sum_{i=1}^{N} C_i \left[(x-x_i)^2 + (y-y_i)^2\right] \ln\left[(x-x_i)^2 + (y-y_i)^2\right] + Ax + By + D, \quad (3)$$

where $C_1, C_2, \ldots, C_n$, A, B, D = coefficients derived from the equations (to calculate the coefficients, matrices are made on the basis of existing anthropometric coordinates defined from the digital head model):

$$\phi(x_i y_i) = f_i \quad i = \overline{1,N}, \quad (4)$$

$$\sum_{i=1}^{N} C_i = 0, \quad (5)$$

$$\sum_{i=1}^{N} C_i x_i = 0, \quad (6)$$

$$\sum_{i=1}^{N} C_i y_i = 0. \quad (7)$$

The resulting equation allows you to set the shape of the surface of the dust respirator half-mask on the control points, which in our case are used as interpolation nodes and correspond to the key anthropometric dimensions of the worker's face. The shape of the spline function describing the surface of the dust respirator half-mask (Figure 5) is given by the polygonal model of the worker's face and is determined by 3D coordinates, which are formed by key anthropometric facial features and depend on the gender, age and facial expressions of the person when performing production operations, and are also the main prerequisite for improving the design of the dust respirator half-mask.

Through the use of the iterative algorithm known as the Iterative Closest Point method (ICP-method), based on

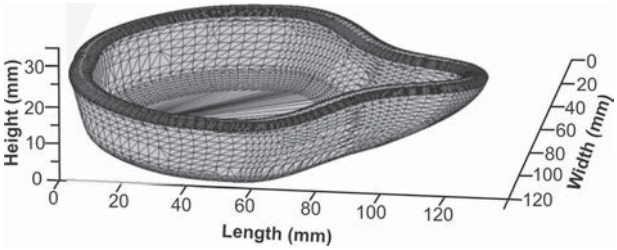

Figure 5. View of the surface of the dust respirator half-mask, built using the spline function.

the iterative procedure of 3D surfaces S_1, S_2 that is based on minimizing the distance between the points of these surfaces, which are compared as objects of linear space $p(S_1, S_2)$, and the probability of coincidence is the norm $||S_1 - S_2||$ in this space, taking into account the difference between the sizes of grid faces and half-masks, surfaces can be estimated by the following formula:

$$(S_1, S_2) = k_{n1} \sum_{i=1}^{N_1} \sum_{j=1}^{N_1} (n_i^1, n_j^1) \cdot e^{-\frac{(c_i^1 - c_j^1)^2}{\sigma^2}} + k_{n2} \sum_{i=1}^{N_2} \sum_{j=1}^{N_2} (n_i^2, n_j^2) \cdot e^{\frac{-(c_i^2 - c_j^2)^2}{\sigma^2}} - 2k_{n1} \cdot k_{n2} \sum_{i=1}^{N_1} \sum_{j=1}^{N_2} (n_i^1, n_j^2) \cdot e^{\frac{-(c_i^1 - c_j^2)^2}{\sigma^2}}, \quad (8)$$

where S_i = centroid of the triangle; k_1, k_2 = coefficients that take into account the mismatch of points on the face and half-masks; N_1, N_2 = number of points in the original 3D surfaces S_1, S_2; n_i = vector of the normal to the ith triangle, the length of which is equal to the area of this triangle; σ = surface area of the triangle.

Table 2 presents the calculated areas of adhesion of the dust respirator half-mask to the worker's face for two different options, the difference between which was the choice of key points that determine the width (for the first it was

Table 2. Results for calculation of the contact area of the dust respirator half-mask for a worker's face.

Option	Obturator area in accordance with parts of a worker's face (cm^2)				Total contact area (cm^2)	Average obturator thickness (cm)
	Nose bridge	Right cheek	Left cheek	Chin		
1	4.2	21.3	20.9	10.8	57.2	0.9
2	3.2	13.4	12.8	9.3	38.7	0.6

assessed by the lower part of the face, and for the second was based on lip length).

To provide the theoretical calculation of protective action of the dust respirator, the mathematical model was created describing the motion of dust-laden flows, both at the surface of the dust respirator half-mask taking into account leaks of air through possible gaps (formed between the obturation line and the worker's face) and inside the encapsulated particle filter, depending on its volume, that differs from the existing one – this takes into account the geometric parameters of the half-mask and encapsulated particle filter.

The movement of the dust aerosol near the surface of the dust respirator half-mask can be represented by two flows (Figure 6). The first enters the encapsulated particle filter and can be described by four differential equations with first-order partial derivatives with Euler variables, which create the equation of continuity of the flow and allow one to obtain the relationship between the kinematic and geometric parameters of the particle filter [21]:

$$\begin{cases} \frac{1}{r}\rho V_r + \frac{\partial \rho}{\partial r}V_r + \frac{\partial V_r}{\partial r}\rho + V_z\frac{\partial \rho}{\partial z} + \frac{\partial V_z}{\partial z}\rho = 0; \\ V_r\frac{\partial V_r}{\partial r} + V_z\frac{\partial V_r}{\partial z} - \frac{V_\theta^2}{r} = k_\phi \cdot V_r - \frac{1}{\rho}RT\frac{\partial \rho}{\partial r}; \\ V_r\frac{\partial V_\theta}{\partial r} + V_z\frac{\partial V_\theta}{\partial z} + \frac{V_r V_\theta}{r} = k_\phi \cdot V_\theta; \\ V_r\frac{\partial V_z}{\partial r} + V_z\frac{\partial V_z}{\partial z} = k_\phi \cdot V_z - \frac{1}{\rho}RT\frac{\partial \rho}{\partial z}, \end{cases} \quad (9)$$

where V_r, V_θ, V_z = projections on the speed vector on the corresponding coordinate axes (m/s); ρ = density of the dust flow in the particle filter element (kg/m^3); k_n = coefficient of penetration (1/s); R = universal gas constant (J/[kg × K]); T = temperature of the dust-laden flow (K). Note: r, z, θ = the coordinates of a point in a cylindrical coordinate system.

The second flow is directed into the gaps that are formed between the obturation line of the half-mask and the surface of the worker's face and can be represented by a known function of the current of the air flow sucked into the gap [22]. If the total area of the gap is calculated using the formula that determines the equivalent radius, then the coefficient of aerosol suction A through the gap

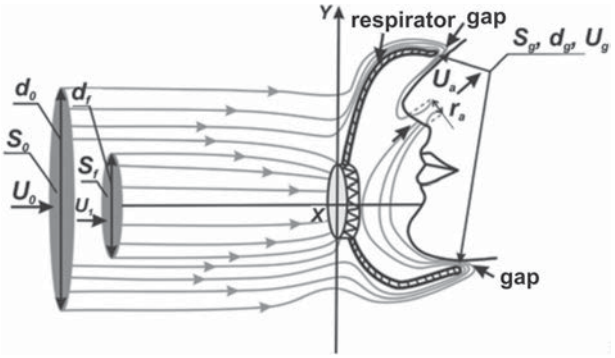

Figure 6. Design scheme of the half-mask of the dust respirator, which is flown around by the flow of dust-laden air. Note: diagram shows the dimensions of the areas with their diameters S_0 and d_0, the air flow that enters the filter and the gap S_g and d_g, air flow only up to the particle filter S_f and d_f, total flow rate U_0 and flow rate in the gap U_g, U_1 = speed of air flow through filter; U_a = speed of airflow in the nasal canal; r_a = radius of the nasal canal.

can be determined by the following formula:

$$A = \frac{U_0 \cdot S_g}{Q_g} = \frac{S_g\sqrt{R_a^2 + (St_a/Fr^2)^2}}{\pi \cdot R_a^2}, \quad (10)$$

where U_0 = air velocity at the surface of the half-mask (m/s); S_g = area of the gap (m^2); Q_g = air flow through the gap (m^3/s); $R_a = U_0/U_g$ = ratio of the velocities of the aerosol near the half-mask of the dust respirator and in the gap; St_a = Stokes number:

$$St_a = \frac{\delta^2 \cdot \rho_p \cdot U_g}{18\mu \cdot d_{eqv}} \quad (11)$$

U_g = air velocity in the gap (m/s); Fr = Froude number:

$$Fr = \frac{U_g}{\sqrt{g \cdot d_{eqv}}}; \quad (12)$$

g = acceleration of free fall (m/s^2); d_{eqv} = equivalent diameter of the gap (m).

Solving the system of Equation (8) using the method of least squares, finite elements and local variations in the corresponding software environment allows one to obtain the dependence of the distribution of the air flow velocity over the volume of the encapsulated particle filter taking into

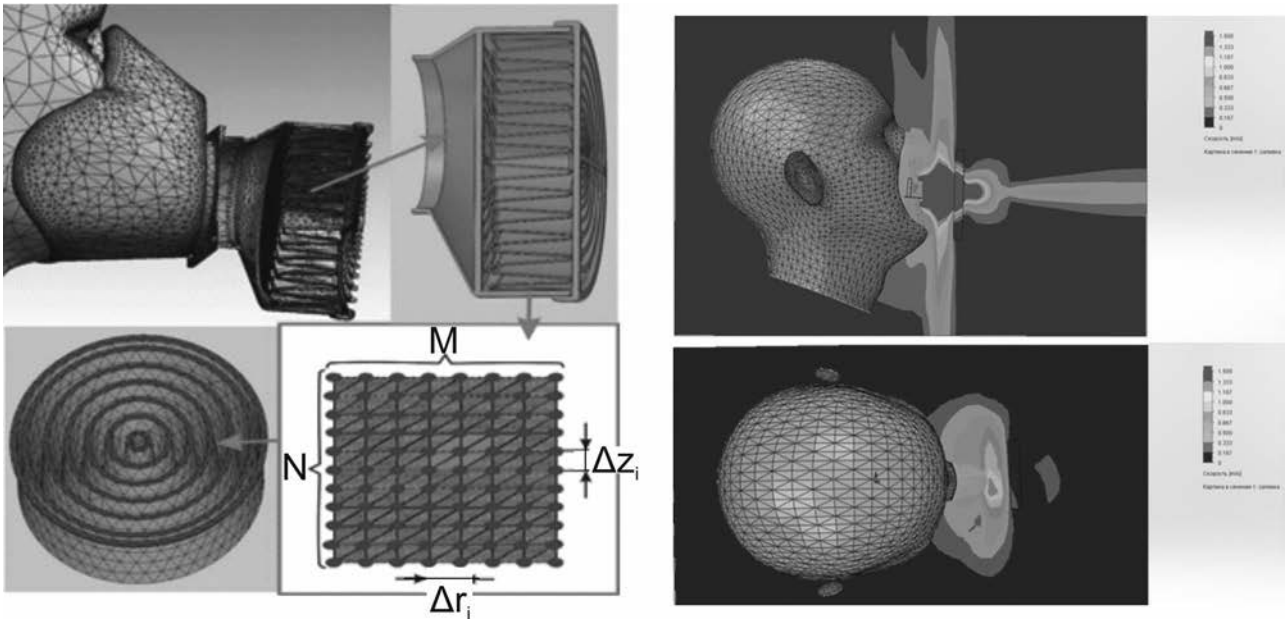

Figure 7. Design scheme of the dust respirator half-mask with an encapsulated particle filter. Note: M = size of the section; N = triangular finite elements; Δr_i, Δz_i = marking of the particle filter section.

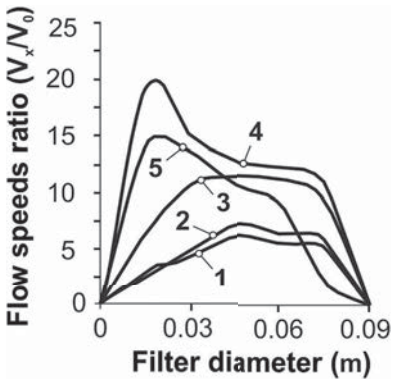

Figure 8. Distribution curves of the relative filtration rate over the diameter of the encapsulated particle filter with an outlet offset by 5 mm (1), 10 mm (2), 15 mm (3) and 20 mm (4) and 25 mm (5) from the center of the box. Note: V_0 = speed of average filtration through the filter, V_x = the filtering speed on the calculated section of the filter, which lays at a distance x from the coordinate origin.

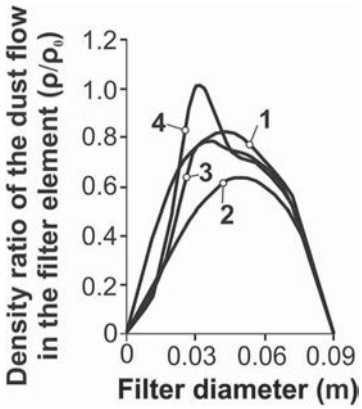

Figure 9. Curves of dependence of distribution of relative density of the dust-gas stream over the area of the filtering element with an outlet offset by 5 mm (1), 10 mm (2), 15 mm (3) and 20 mm (4) from the center of the box. Note: ρ_0 = the average density of dust and gas flow in the plane of the filter, ρ_x = the density of dust and gas flow in the calculated section of the filter with a given plane, which is at a distance x from the coordinate origin.

account its geometric parameters (Figure 7), and to estimate their influence on the coefficient of penetration of the encapsulated particle filter and the suction of air between the gaps formed between the half-mask obturation line and the surface of the worker's face (Figures 8 and 9).

The conducted research allowed one to systematize the existing approaches to the design of half-masks and to create an algorithm for RPE development (Figure 10), which differs from the existing ones by estimating the parameters of the polygonal model of the head, checking the area of adhesion of the designed model of the half-mask to the prototype and the preliminary calculation of the protection factor.

3. Results

3.1. *Results of theoretical research*

The dependences of the protective properties of the RPE from the coefficients of the particle filter penetration and velocity distribution of air flow across the volume of the encapsulated particle filter obtained as a result of the calculation allow one to evaluate the influence on ergonomics of dust respirators caused by geometrical parameters of the latter (height and diameter of the encapsulated particle filter, inlet and outlet diameters, particle filter height and diameter, outlet offset from the center of the box). Also,

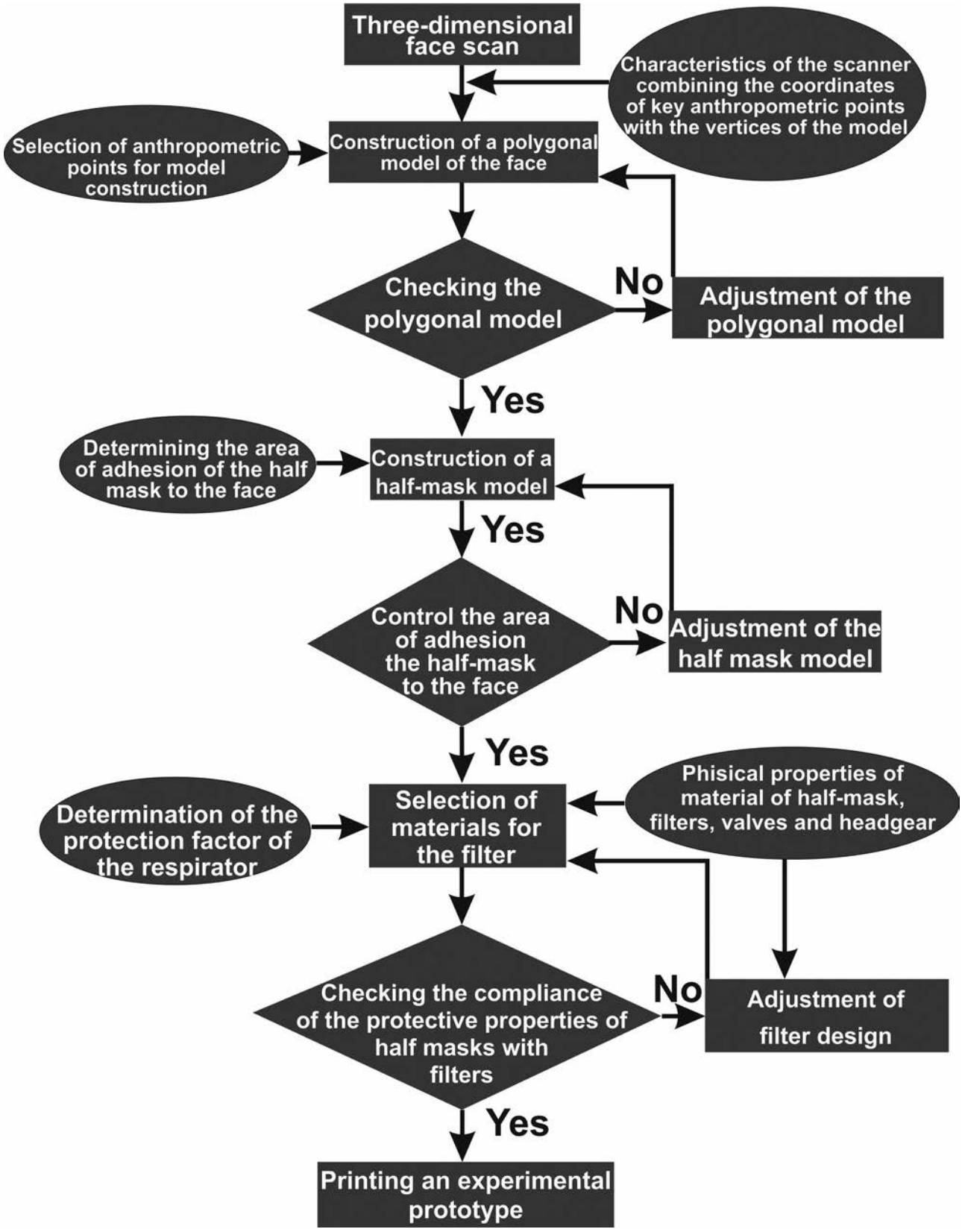

Figure 10. Algorithm for designing half-masks.

Table 3. Calculated data for the protection coefficient of the dust respirator half-mask with different sizes of gaps between the half-mask obturation line and the surface of a worker's face.

Gap diameter (mm)	Suction gap area, S_g (mm^2)	Air flow through the gap, Q_g (ml/min)	Total pressure difference across the respirator, Δp (Pa)	Protection factor, PF
1	3.1	424.1	69.4	20.3
2	14.6	811.1	56.8	11.8
3	19.7	882.5	53.8	9.3
4	28.3	1021.1	47.5	6.7

on their basis, the value of the protection factor of dust respirators was clarified, taking into account the suction through the gaps between the half-mask obturation line and the surface of the worker's face:

$$K_d = [k_{cf} + k_n \cdot (A - k_{cf})]^{-1}, \quad (13)$$

where PF = protection factor of dust respirator; k_{cf} = coefficient of aerosol penetration through the particle filter; A = coefficient of aerosol suction through the gap; $k_n = Q_g/Q_f$ = coefficient of penetration; Q_g = air flow due to leaks in the obturation band of the respirator (dm^3/min); Q_f = air flow through the particle filter (dm^3/min).

The difference between this method of calculating the protective effectiveness of the dust respirator from the existing one is that it takes into account the variability of the size of the gap between the half-mask obturation line and the surface of the worker's face using the suction coefficient through the ratio of the parameter R_a, and taking into account the influence of geometric parameters of encapsulated particle filters on the protection factor PF (Table 3).

The analysis of the obtained dependences allowed determining ways to improve the distribution of air flow over the particle filter area. Thus, changing the location and size of the outlet relative to the center of the box allows for uniform settling of dust on the particle filter surface (Figure 11). It was established that the pressure drop on the encapsulated particle filters of dust respirators was determined not only by the coefficient of resistance of particle filters and air flow through them, but also by the ratio of the diameters of its outlets and inlets, with its minimum value being in the range of 0.4 to 0.8.

A similar effect can be obtained by making the rear wall of the encapsulated particle filter in the form of a dust respirator converging cone (Figure 12). This allows gradually increasing the speed of the air flow on the way to the intake valve through the decrease in the area of the cone cross-section, which contributes to a uniform flow over the corrugated surface of the particle filter. This distribution of the air flow provides, in comparison with the known designs of encapsulated particle filters, a slight increase in the breathing resistance on the particle filter under dust contamination conditions and increases the protective action period of the dust respirator. Figure 13 shows the industrial sample of the dust respirator.

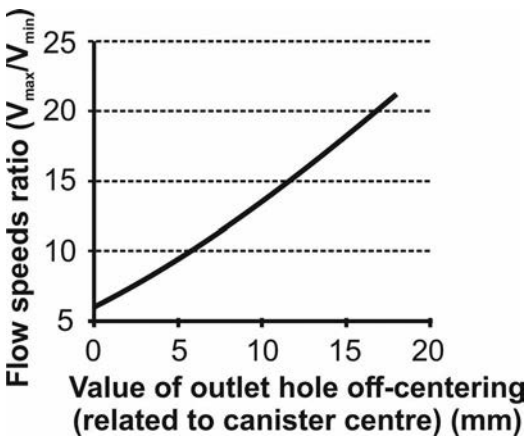

Figure 11. Distribution curve of air flow relative velocity and value of the outlet offset of a dust respirator encapsulated particle filter. Note: V_{max} = the maximum filtration speed recorded at the calculated section of the filter, V_{min} = the minimum filtration velocity at the calculated section of the filter.

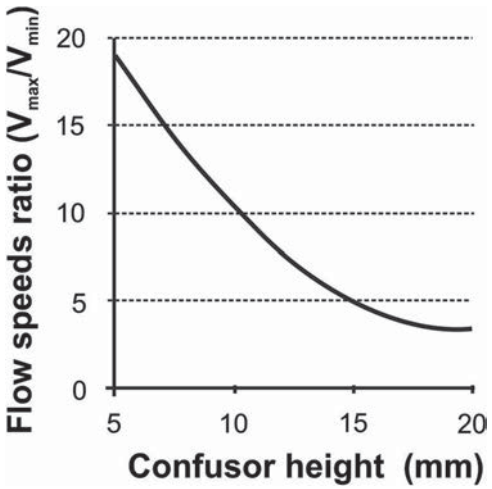

Figure 12. Distribution curve of air flow relative velocity and the height of the dust respirator converging cone. Note: V_{max} = the maximum filtration speed recorded at the calculated section of the filter, V_{min} = the minimum filtration speed at the calculated section of the filter.

Figure 13. Industrial design of a dust respirator.

3.2. *Results of experimental research*

3.2.1. *Investigation of the increase in particle filter pressure drop during dust pollution*

The experimental research was carried out on a special test stand (Figure 14).

The cross-sectional area of the test chamber is – 0.4 m^2, as required by the procedure according to the requirements of Standard No. EN 13274-8:2005. The concentration of dolomite dust was provided equal to 500 ± 50 mg/m^3. The time of dust contamination was determined by the achievement of the finite pressure difference at the half-masks in accordance with the requirements of Standard No. EN 143:2000/A1. Using the ejector 3 and the compressor 1 at an air flow rate of 60 m^3/h, the dolomite dust was fed from the dust generator 10 through the diffuser 4 and dust distributor 11 to the test chamber 13. The diffuser and distributor in the test stand design ensure uniform distribution of dust and air flow over the chamber height. The air flow in the chamber is controlled by the flow meter 6. To remove dust from the chamber and protect the environment, the exhaust fan 7 with the cyclone 5 is installed.

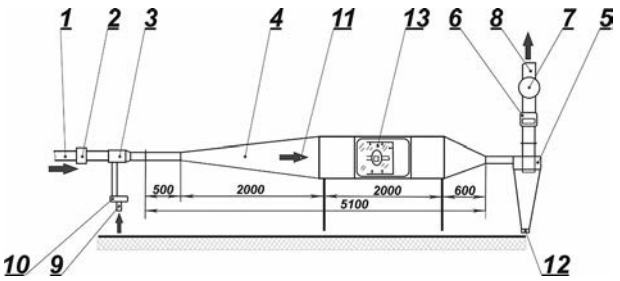

Figure 14. General view of the test stand. Note: 1, 9 = compressed air supply; 2 = prefilter for compressed air treatment; 3 = ejector; 4 = diffuser; 5 = cyclone; 6 = flow meter; 7 = exhaust fan; 8 = outlet pipe;10 = dust generator; 11 = dust distributor; 12 = damper; 13 = test chamber.

The half-mask of the dust respirator was installed on a dummy head and placed in the test chamber. The dummy head has a special tube mounted onto it through which the connection with the breathing machine is ensured, and there is a micromanometer connected to monitor changes in the pressure drop. In accordance with the requirements of Standard No. EN 143:2000/A1, the breathing machine has been set to a frequency of 15 cycles/min and 2 dm^3/stroke. In addition, the air was humidified and heated to 37 °C using a Boneco ('Plaston AG', Switzerland) adjustable ultrasonic humidifier. Temperature and humidity control was ensured by TXA ('DigiTOP.UA' LLC, Ukraine) sensors.

To determine the dust concentration, a constant volume of air at an flow rate of 2 dm^3/min was drawn through the AFA VP-10 (Spetskhimpostach-D, LLC, Ukraine) particle filter using an aspirator. The allonge for fixing the AFA VP-10 particle filter is placed in the middle of the chamber near the test sample. The concentration of dust in the chamber was determined using the following formula:

$$C = \frac{10^3 \cdot (m_2 - m_1)}{Q \cdot t}, \tag{14}$$

where C = concentration of dust; m_2 = weight of the AFA VP-10 particle filter with dust after sampling (mg); m_1 = weight of the AFA VP-10 particle filter (mg); Q = air flow (dm^3/min); t = time of air sampling (min).

The initial mass of AFA VP-10 particle filters having diameter 36 mm before and after the study with sedentary dust was checked on VLO 200 laboratory scales ('GOSMETR' SPE, Russia). Time was controlled by an HS 43 electronic stopwatch ('Standard-M', SPE LLC, Ukraine). The pressure difference was controlled using an MKV 250

compensating micromanometer ('Standard-M', SPE LLC, Ukraine) and calculated by the following formula:

$$R = (n_i - n_0) \cdot K_1, \tag{15}$$

where R = pressure difference; n_i = micromanometer reading after the encapsulated particle filter of the dust respirator (Pa); n_0 = initial resistance of the measuring system (Pa); K_1 = correction factor when measuring temperature and atmospheric pressure.

The experimental models of dust respirators were equipped with a particle filter cartridge with a particle filter (type 1), which consisted of a cylindrical body with an offset outlet relative to the central axis of the particle filter; a particle filter cartridge with a cylindrical body with its outlet located at the center of the particle filter (type 2); and a particle filter cartridge (type 3), which consisted of a cylindrical body with its rear wall made in the form of a truncated cone with an outlet, where there was the respiration valve. The cartridges had identical corrugated polypropylene particle filters inside. FRPA P2 particle filters ('Standard-M', SPE LLC, Ukraine) corresponding to the second class of protection were used in the experiment.

Three particle filters were installed in each encapsulated particle filter and the average value of the pressure drop was determined. A total of 168 measurement results were obtained. The obtained results were used to determine the uncertainty of measurements at $p < 0.05$ in accordance with Standard No. JCGM 100:2008, 'Evaluation of measurement data – Guide to the expression of uncertainty in measurement'.

The results of laboratory tests of the dust respirator showed that the initial respiratory resistance of the encapsulated particle filter with the converging cone was almost 25% less than in other boxes; at the same time, the dust capacity and the protective action period were increased more than twice with a concentration of dust in the air of 500 mg/m^3 (Figure 15).

Table 4 presents the results for the studies of the dust respirator with different types of particle filter cartridges.

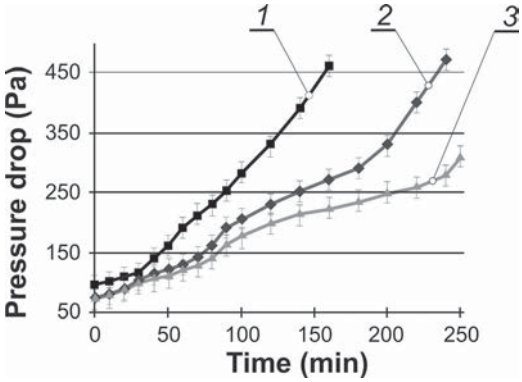

Figure 15. Dependence of pressure difference on the dust respirator particle filters from the time of dust contamination, with a concentration of 300 mg/m^3 and air flow rate of 95 dm^3/min located in the encapsulated particle filter with outlet diameter 32 mm: 18 mm off-center (1), no offset (2) and rear wall in the form of a converging cone (3).

3.2.2. *Study of the protective effectiveness of particle-filtering respiratory protective devices*

The protective efficiency of the filtering respiratory protective devices was tested on a special stand (Figure 16), which complies with Standard No. EN 140:1998/AC:1999. It consists of an ultrasonic test aerosol generator, a test chamber where the tester was located and a Selmi C-115E spectrophotometer ('SELMI', LLC, Ukraine) with a built-in aspirator for sampling. As a test aerosol 0.1% sodium chloride solution was used, which was dried and fed with an air flow rate of 100 dm^3/min in the test chamber. The test aerosol generator provided the distribution of aerosol particles in the range from 0.02 to 2 μm with a weight average diameter of 0.6 μm. The uniformity of its distribution in the test chamber was ensured by ventilation systems and test aerosol supply. The concentration in the breathing zone of the tester during the studies was constantly monitored and was 8 ± 4 mg/m^3. To measure the concentration under the respirator mask, a special sampler was used, which sucked air between the nose and lips. In the

Table 4. Results for studies of the dust respirator with different types of particle filter cartridges.

	Encapsulated particle filter type		
Variable	Type 1	Type 2	Type 3
Initial pressure drop on the particle filter element (Pa)	71.2 ± 3.2	72.3 ± 3.5	70.5 ± 3.3
Initial pressure drop on the encapsulated particle filter (Pa)	85.2 ± 3.1	78.8 ± 3.3	75.4 ± 3.1
Dust holding capacity (g)	1.2 ± 0.051	1.3 ± 0.025	2.4 ± 0.452

Note: type 1 = particle filter cartridge with a particle filter, consisting of a cylindrical body with an offset outlet relative to the central axis of the particle filter; type 2 = particle filter cartridge with a cylindrical body with its outlet located at the center of the particle filter; type 3 = particle filter cartridge, consisting of a cylindrical body with its rear wall made in the form of a truncated cone with an outlet, where there was the respiration valve.

Table 5. Dimensions of the faces of the participants in the experiment.

Face height (mm)	Face width (mm)		
	129–139 (zone 1)	140–145 (zone 2)	146–155 (zone 3)
136–126	1 tester	2 tester	–
125–116	1 tester	2 tester	1 tester
115–105	–	2 tester	1 tester

chamber, air samples with an aerosol were taken simultaneously with the sampling from the area under the respirator. The concentration chamber was located at the level of the tester's face. The suction rate of air in both the first and second cases was 1.5 dm^3/min. During the tests, the respirator was equipped with an FRPA P2 particle filter, a second class of protection, which met the requirements of Standard No. EN 143:2000/A1, i.e., the penetration rate of the test aerosol was no more than 6%. The study determined the overall protection factor of the respirator using the following formula:

$$PF = \frac{100}{K_p}, \tag{16}$$

where PF = protection factor; K_p = penetration coefficient of the test aerosol, which consists of the penetration of the aerosol through the particle filter and through the sealing strip between the face and the half-mask.

The test involved 10 volunteers (European race), four women and six men aged 23–44 years according to the parametric size of the face (Table 5), who were previously instructed on the proper use of a filtering respiratory protective device and checking the correctness of its fit to the face. If in the process of testing there was a need to adjust the mounting of the half-mask, then there was a stop fixing the value of the submask concentration of the test aerosol, which was continued after restoring the initial parameters of the system.

During the study, the testers performed sequentially the exercises provided for in Standard No. EN 140:1998/AC:1999: normal breathing; deep breathing; head movements from side to side; head movements up and down; conversation aloud; walking on a treadmill at a speed of 6 km/h. Each exercise was performed for 2 min. Each examiner made three measurements for each exercise. The result was averaged and entered into a special table in the 'Atomic Absorption Spectroscopy program' (AAS-2009, version 2), which provides for the definition of statistics in accordance with Standard No. ISO 5725-6: 1994. The results of the study are presented in Table 6.

The results of the study of the protective effectiveness of the filtering respiratory protective devices on volunteers showed compliance of the developed design with the second class of protection in accordance with Standard No. EN 140:1998/AC:1999, and the suction coefficient was no more than 5%. This can be verified by determining the minimum protection factor, taking into account the maximum allowable value of the absorption coefficient of the respirator and the penetration factor of the particle filter, which is respectively not less than 9%.

However, another result is interesting: the worst rates were recorded among testers with a small face size, who are in the first zone (protection factor did not exceed 15%),

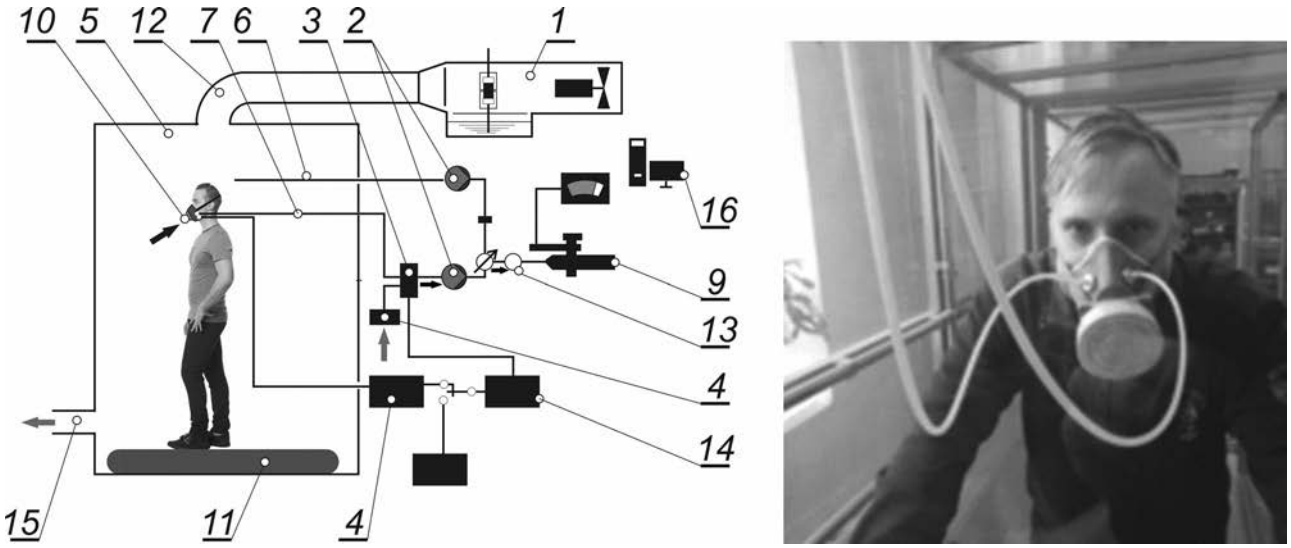

Figure 16. Scheme of the stand for determining the coefficient of penetration of respirators by test aerosol on humans. Note: 1 = aerosol generator with compressor and aerosol line; 2 = aspirator; 3 = multiway valve; 4 = particle filter; 5 = test chamber, which receives aerosol from above; 6 = branch pipe for sampling of test aerosol from the chamber; 7 = branch pipe for sampling of test aerosol from the submask space; 8 = pressure sensor; 9 = spectrophotometer; 10 = dust respirator; 11 = treadmill located in the test chamber; 12 = air duct and air distributor; 13 = branch pipe for pure air; 14 = system of distribution of phases of inhalation–exhalation; 15 = exhaust ventilation; 16 = PC.

Table 6. Results for an experimental test of a filtering respiratory protective device.

Tester	Coefficient of protection (*PF*) of the filtering respiratory protective device when performing standard exercises					Average protection factor *PF* (%)
	Normal breathing	Head movements from side to side	Head movements up and down	Conversation aloud	Walking on a treadmill	
1	16.1	15.2	14.2	15.5	14.2	14.8 ± 0.6
2	17.5	16.6	15.1	14.5	16.1	15.6 ± 0.8
3	22.3	19.3	20.2	18.4	19.2	19.6 ± 1.1
4	23.3	19.4	18.3	17.3	20.3	19.4 ± 1.6
5	25.1	24.1	22.5	18.4	19.4	21.6 ± 2.4
6	23.4	21.4	20.1	16.7	17.1	19.4 ± 2.3
7	18.7	17.5	15.6	14.6	15.5	15.8 ± 1.3
8	20.2	20.5	18.8	15.4	17.8	18.0 ± 1.6
9	16.6	15.3	13.4	12.2	14.2	14.0 ± 1.2
10	16.8	15.9	16.6	12.6	14.3	14.6 ± 1.3

and a quite large size (third zone), where the protection factor was equal to 14%, which indicates the appearance of gaps along the strip of the seal, which are mostly formed due to specific movements of the head and the need for user conversation. The obtained figures are natural, because the half-mask was designed based on the average size of the faces, which does not allow equal protection for all users. It is important to provide at least three sizes of half-mask (which are now practiced by all manufacturers). However, we believe that the rational number of sizes, based on research, should be five. In this way, reliable protection of employees can be ensured.

4. Discussion

As a result of the performed work, the algorithm for designing and manufacturing filter masks of the dust respirator, which consists of several stages, was worked out and improved. In the first stage, the dimensions of faces of potential consumers were defined, and then the dimensions obtained were applied to a 3D head model on which the contour of a half-mask obturator was constructed. We paid attention to the difficulties that were associated with different thickness and elasticity of different parts of the face, which could affect the obturator design to ensure uniformity of clamping forces and minimal impact on blood circulation in the soft tissues of the worker's face. Then, we selected the appropriate dust respirator structure (number of particle filter layers, needed respiration valve) depending on the concentration and properties of aerosols and operating conditions and the type of particle filter material depending on the characteristics of harmful aerosols (diameter of aerosol particles, toxicity, hazard class). This process was described in detail by Makowski and Okrasa [23] and by Hayashi and Tokura [24]. It should be noted that the modern development level of particle filter materials allows for a high degree of air purification.

The resulting experimental model of the dust respirator is pre-checked for protective properties in terms of air suction through the gaps on the obturation line. The quality of the dust respirator half-masks at the design stage is evaluated for the effectiveness of each individual element, which is included in the design mainly theoretically. The problem is that, unfortunately, there is no adequate theoretical model of RPE to accurately calculate the protective properties of dust respirator half-masks. Unfortunately, the proposed approaches require experimental data to clarify various calculated coefficients [25,26]. This greatly complicates the process of checking, which can be carried out accurately on already manufactured samples. In this case, the inspection requires about two dozen finished products. It is also quite difficult to quickly change the design to obtain the necessary parameters. The proposed algorithm differs from the known ones by the presence of preliminary verification of protective properties – after each design stage. This test is quite simple, and its results allow you to quickly introduce adjustments to the 3D model of the dust respirator half-mask.

5. Conclusion

- As a result of the research, an algorithm for designing a half-mask and an encapsulated particle filter of an antidust respirator is offered that differs from existing algorithms by the existence of a check of efficiency of the half-mask at a design stage: estimation of parameters for a polygonal model of the head, checking the area of adhesion of the designed model of the half-mask to the prototype and preliminary calculation of the protection factor.
- A mathematical model has been developed that describes the movement of dust streams near the surface of the half-mask and in the encapsulated particle

filter of a dust respirator, which allows one to establish the dependence of air flow velocity distribution in the encapsulated particle filter of a dust respirator and evaluate the protective properties of respirators.

- The rational geometrical parameters of the encapsulated particle filter of the dust respirator are determined. The transition from the particle filter to the inlet valve opening is made in the form of a confuser; its height, inlet diameter and displacement of the opening from the center of the encapsulated particle filter are substantiated.
- It is determined that the protection factor of the filtering respiratory protective devices with particle filters of the second class of protection ranged from 14 to 21.6%, indicating a rather small size of the gaps in the seal strip, which are mostly formed due to specific head movements and the need for user conversation. Although all of the tested filtering respiratory protective devices met the stated values, there is still concern about the minimum values of volunteers with certain facial features, which requires the development of five sizes of half-masks.

Acknowledgements

The authors gratefully acknowledge Maksym Vasylchenko for the opportunity to conduct experimental research presented in the article

The authors thank the editors for providing the opportunity to present the research results on the pages of this respectable journal as well as the reviewers for providing valuable assistance in improving the scientific article representation quality.

Disclosure statement

No potential conflict of interest was reported by the authors.

ORCID

Serhii Cheberyachko http://orcid.org/0000-0003-3281-7157
Yurii Cheberyachko http://orcid.org/0000-0001-7307-1553
Mykola Naumov http://orcid.org/0000-0002-9748-2506
Oleg Deryugin http://orcid.org/0000-0002-2456-7664

References

[1] Kirillov VF, Bunchev V, Chirkin . O sredstvakh individual'noy zashchity organov dykhaniya rabotayushchikh (obzor literatury) [On means of individual protection of respiratory organs of the workers (literature review)]. J Occup Med Ind Ecol. 2013;4:25–31. Russian.
[2] Cheberyachko SI, Frundin V, Cheberyachko Y, et al. Studying the influence of a filter box design on respirator resistance to breathing. J Int Soc Respir Prot. 2017;34(1):58–64.
[3] Oestenstad RK, Elliot LJ, Beasley TM. The effect of gender and respirator brand on the association of respirator fit with facial dimensions. J Occup Environ Hyg. 2007;4(12):923–930. doi:10.1080/15459620701709619
[4] Lei Z, Yang J, Zhuang Z. A novel algorithm for determining contact area between a respirator and a headform. J Occup Environ Hyg. 2014;11(4):227–237. doi:10.1080/15459624.2013.858818
[5] Golinko VI, Cheberyachko SI, Chirkin OV. 'Zakhyst bez zakhystu'. Rekomendatsiyi vchenykh shchodo stvorennya prohram respiratornoho zakhystu pratsyuyuchykh ['Protection without protection'. Recommendations of scientists on creation of respiratory protection programs for workers]. Labour Protection. 2015;4:52–54. Ukrainian.
[6] Janssen LL, Weber R. The effect of pressure drop on respirator faceseal leakage. J Occup Environ Hyg. 2005;2(7):335–340. doi:10.1080/15459620590965068
[7] Yu-Mei K, Chane-Yu L, Chih-Chieh C, et al. Evaluation of exhalation valves. Ann Occup Hyg. 2005;49(7):563–568.
[8] Wood GO. Estimating service lives of organic vapor cartridges II: a single vapor at all humidities. J Occup Environ Hyg. 2004;1:472–492. doi:10.1080/15459620490467792
[9] Lei Z, Yang JJ, Zhuang Z. Headform and N95 filtering facepiece respirator interaction: contact pressure simulation and validation. J Occup Environ Hyg. 2012;9:46–58. doi:10.1080/15459624.2011.635130
[10] Gutierrez AMJA, Melissa DG, Seva RR, et al. Designing an improved respirator for automotive painters. Int J Ind Ergon. 2014;44(1):131–139. doi:10.1016/j.ergon.2013.11.004
[11] Zhuang Z, Bradtmiller B, Shaffer RE. New respirator fit test panels representing the current U.S. civilian work force. J Occup Environ Hyg. 2007;4(9):647–659. doi:10.1080/15459620701497538
[12] Groce D, Guffey S, Viscusi DJ, et al. Three-dimensional facial parameters and principal component scores: association with respirator fit. J Int Soc Respir Prot. 2010;27(1):1–15.
[13] Brosseau LM. Fit testing respirators for public health medical emergencies. J Occup Environ Hyg. 2010;7(11):628–632. doi:10.1080/15459624.2010.514782
[14] Plebani C, Listrani S, Di Luigi M. Facciali filtranti: effetto dell'accumulo di aerosol oleoso sulla penetrazione attraverso il materiale filtrante [Filtering facepieces: effect of oily aerosol load on penetration through the filtering material]. Med Lav. 2010;101(4):293–302. Italian.
[15] Cai M, Li H, Shen S, et al. Customized design and 3D printing of face seal for an N95 filtering facepiece respirator. J Occup Environ Hyg. 2018;15(3):226–234. doi:10.1080/15459624.2017.1411598
[16] Stechkina IB, Kirsh VA. Optimization of parameters of filters in a multistage system of fine gas filtration. Theoret Found Chem Eng. 2003;37(3):218–225. doi:10.1023/A:1024071202844
[17] Stechkina IB, Kirsh VA. Kinetics of the clogging and optimization of prefilters in a two-stage air cleaning system. Theoret Found Chem Eng. 2010;44(1):238–245.
[18] Kovacs L, Zimmermann A, Brockmann G, et al. Three-dimensional recording of the human face with a 3D laser scanner. J Plast Reconst Aesth Surg. 2006;59(11):1193–1202. doi:10.1016/j.bjps.2005.10.025.
[19] Dunnett SJ, Vincent JH. A mathematical study of aerosol sampling by an idealised blunt sampler oriented at an angle to the wind: the role of gravity. J Aerosol Sci. 2000;31(10):1187–1203. doi:10.1016/S0021-8502(00)00024-0
[20] Chen W, Zhuang Z, Benson S, Du L, Yu D, Landsittel D, Wang L, Viscusi D, Shaffer RE. New respirator fit test panels representing the current Chinese civilian workers. Ann Occup Hyg. 2009;53(3):297–305. doi:10.1093/annhyg/men089
[21] Galeev RS, Zaripov SK. A theoretical study of aerosol sampling by an idealized spherical sampler in calm air. J Aerosol

Sci. 2003;34(9):1135–1150. doi:10.1016/S0021-8502(03)00091-0

[22] Yumiao C, Jianping W, Zhongliang Y. The human factors/ergonomics studies for respirators: a review and future work. Int J Clothing Sci Technol. 2015;27(5):652–676. doi:10.1108/IJCST-06-2014-0077

[23] Makowski K, Okrasa M. Application of 3D scanning and 3D printing for designing and fabricating customized half-mask facepieces: a pilot study. Work. 2019;63(1):125–135. doi:10.3233/WOR-192913

[24] Hayashi C, Tokura H. The effects of two kinds of mask (with or without exhaust valve) on clothing microclimates inside the mask in participants wearing protective clothing for spraying pesticides. Int Arch Occup Environ Health. 2004;77(1):73–78. doi:10.1007/s00420-003-0472-3

[25] Huang XJ, Ge D, Xu ZK. Preparation and characterization of stable chitosan nanofibrous membrane for lipase immobilization. Eur Polym J. 2007;43(9):3710–3718. doi:10.1016/j.eurpolymj.2007.06.010

[26] Lee HP, Wang DY. Objective assessment of increase in breathing resistance of N95 respirators on human subjects. Ann Occup Hyg. 2011;55(8):917–921. doi:10.1093/annhyg/mer065